

1

2

3 **Determination of Dacarbazine Φ -order photokinetics, quantum**
4 **yields and potential for actinometry.**

5

6

Mounir Maafi*, Lok-Yan Lee

7

8

9

Leicester School of Pharmacy, De Montfort University, The Gateway, Leicester LE1 9BH, UK

10

11

12 **Abstract**

13 The characterization of drugs' Photodegradation kinetics is more accurately achieved by means
14 of the recently developed Φ -order kinetics than by the 0th-, 1st- and/or 2nd-order classical
15 treatments. The photodegradation of anti-cancer Dacarbazine (*DBZ*) in ethanol has been
16 investigated and found to obey Φ -order kinetics when subjected to continuous and
17 monochromatic irradiation of various wavelengths. Its photochemical efficiency was proven to
18 be wavelength-dependent in the 220-350 nm range, undergoing a 50-fold increase. Albeit this
19 variation was well defined by a sigmoid pattern, the overall photoreactivity of *DBZ* was proven
20 to depend also on the contributions of reactants' and experimental attributes. The usefulness
21 of *DBZ* to serve as a drug-actinometer has been investigated using the mathematical
22 framework of Φ -order kinetics. It has been shown that *DBZ* in ethanol can represent a good
23 candidate for reliable actinometry in the range 270–350 nm. A detailed and easy-to-
24 implement procedure has been proposed for *DBZ*-actinometry. This procedure could
25 advantageously be implemented prior to the determination of the photodegradation quantum
26 yields. This approach might be found useful for the development of many drug-actinometers
27 as alternatives to quinine hydrochloride.

28

29 **Keywords:** Dacarbazine, photodegradation, Φ -order kinetics, quantum yield, actinometry.

30

31 **Corresponding author :**

32 mmaafi@dmu.ac.uk (M. Maafi);

33 Tel.: +44 116 257 7704;

34 fax: +44 116 257 7287.

35 1. Introduction

36

37 Dacarbazine (*DBZ*) is an anti-cancer drug used for the treatment of metastatic malignant
38 melanoma and Hodgkin's disease.¹ It is also sometimes used in combination with other drugs for
39 soft tissue sarcoma.² *DBZ* is supplied as a sterile, lyophilized powder that can be reconstituted
40 for intravenous injection.^{3,4} *DBZ* can also be dispensed orally but this way of administration is
41 limited due to its incomplete absorption in the body.⁵

42

43 The photodegradation of *DBZ* in aqueous solution, when subjected to both sunlight and
44 fluorescent light, has been reported.^{3,6-8} *DBZ* (0.1 mg/mL solutions) was found to rapidly
45 photodegrade (in less than an hour) under the forced irradiation conditions standardly used for
46 photostability testing.^{9,10}

47

48 Despite a large number of studies reported, so far, on the photodegradation and
49 photostabilisation of *DBZ*, only a few included kinetic studies. Nevertheless, the reaction order
50 corresponding to *DBZ* photodegradation is still controversial as it was reported to obey both
51 zero-order¹¹ and pseudo-first-order⁹ kinetics in solution.

52

53 In fact, such an ambiguity on the reaction order, is ubiquitous in pharmaceutical studies in
54 relation to the photodegradation of drugs.^{12,13} In our team, we have recently proposed a new
55 approach based on Φ -order kinetics that was found useful for the description and

56 quantification of unimolecular AB(1 Φ) and reversible AB(2 Φ) photodegradation reactions of
57 drugs¹⁴⁻¹⁸. The Φ -order kinetics solves the uncertainty on drugs photodegradation order for
58 these types of reaction systems.

59

60 In this study, *DBZ* kinetics was investigated in ethanolic solutions using Φ -order kinetics. This
61 tool was employed to screen the change of *DBZ* photodegradation quantum yield in relation to
62 the irradiation wavelength. It was also used to explore and demonstrate the potential of *DBZ* in
63 actinometry.

64

65

66

67

68

69

70

71 **2. Materials and methods**

72

73 2.1. *Materials*

74 Dacarbazine, 5-(3,3-dimethyltriazin-1-yl)imidazole-4-carboamide, (DBZ), and
75 spectrophotometric grade ethanol were purchased from Sigma-Aldrich.

76

77 2.2. *Chromatographic Conditions*

78 Dacarbazine and its photoproducts were separated on a Gemini C₁₈ reverse phase column
79 5 μm, 2.1 x 50 mm (Phenomenex, UK) fitted to a Perkin Elmer Series 200 Pump and UV/Vis
80 Detector, and a 600 Series Link interface; all of which were controlled remotely using
81 TotalChrom software (PerkinElmer, USA). Separation was achieved at a flow rate of 0.5 ml/min
82 with a mobile phase of 70% water (adjusted to pH 3 with glacial acetic acid) and 30%
83 acetonitrile. An injection loop of 20 μl was used and the detector wavelength was set at
84 236 nm. The overall run time of the assay was 10 min. The retention times for DBZ and its
85 photoproduct were 3.87 and 4.21 min, respectively. The linearity range of DBZ calibration
86 graph ranged between 4.8 x 10⁻⁵ M and 5.5 x 10⁻⁴ M.

87

88 2.3. *Monochromatic continuous irradiation*

89 For irradiation experiments, a Ushio 1000 W xenon arc-lamp light source housed in a housing
90 shell model A6000 and powered by a power supply model LPS-1200, was used. This set up was
91 cooled by tap water circulation through a pipe system. The lamp housing was connected to a
92 monochromator model 101 that allows the selection of specific irradiation wavelengths since it

93 consists of a special f/2.5 monochromator with a 1200 groove/mm at 300nm blaze grating. The
94 excitation beam was guided through an optical fibre to impinge from the top of the sample
95 cuvette i.e. the excitation and the analysis light beams were perpendicular to each other. The
96 set up was manufactured by Photon Technology International Corporation.

97

98 2.4. The monitoring system

99

100 A diode array spectrophotometer (Agilent 8453) was used to measure the various absorption
101 spectra and kinetic profiles for the irradiation and calibration experiments. This
102 spectrophotometer was equipped with a 1-cm cuvette sample holder and a Peltier system
103 model Agilent 8453 for temperature control. As such, the sample was kept at 22°C, stirred
104 continuously during the experiment, and completely shielded from ambient light. The
105 spectrophotometer was monitored by an Agilent 8453 Chemstation kinetics–software.

106

107 A Radiant Power/Energy meter model 70260 was used to measure the radiant power of the
108 incident excitation beams.

109

110 The radiant power, given in $\text{mW}\cdot\text{cm}^{-2}\cdot\text{s}^{-1}$ by the radiant power meter, is converted to the
111 appropriate unit ($\text{einstein}\cdot\text{dm}^{-3}\cdot\text{s}^{-1}$) for each wavelength, to be used in Eq.2. Accordingly, the
112 reaction rate-constant ($k_{DBZ}^{\lambda_{irr}}$) is expressed in s^{-1} .

113

114 2.5. *Kinetic data treatment*

115 In order to carry out non-linear fittings and to determine best-fit curves, a Levenberg-
116 Marquardt iterative program within the Origin 6.0 software was used.

117

118 2.6. *DBZ solutions*

119 DBZ stock and diluted solutions were prepared in ethanol, protected from light by aluminium
120 foil wrapping and kept in the fridge while not in use. As such DBZ solutions remained stable for
121 several weeks. The stock solution was diluted to prepare fresh analytical solutions (*ca.* 5×10^{-6}
122 M) for analysis used to perform irradiation experiments at various wavelengths.

123

124 Experiments were conducted at least in triplicates.

125

126

127 **3. Results and discussion**

128

129 **3.1. The Mathematical framework**

130 The long lasting problem of achieving closed-form integration of photoreaction differential
131 equations, has meant that no integrated rate-laws were available to describe photochemical
132 reactions.^{12,19} This situation represents a major issue for photokinetic studies and the reliable
133 quantification of phototransformations.

134

135 However, an expression has previously been established for the photodegradation of an initial
136 species (*A*) into a photoproduct (*B*) via a unimolecular photoreaction involving a single
137 photochemical step ($\Phi_{A \rightarrow B}^{\lambda_{irr}}$), the so-called AB(1 Φ) photoreaction. The closed-form integration
138 was achieved for the case where *A* is the only absorbing species in the reactive medium
139 ($\epsilon_B^{\lambda_{irr}} = 0$).¹⁴ This integrated rate-law was then used as a template to develop a semi-
140 empirical rate-law model for the situation where both (*A* and *B*) species absorb the excitation
141 light, whose reaction differential equation cannot be solved. Optimization, testing and
142 validation of the developed semi-empirical rate-law (Eq.1) were achieved by using data
143 generated by Runge-Kutta numerical integration method.¹⁶

144

145 The general AB(1 Φ) semi-empirical rate-law equation describing the time variation of the
146 cumulative absorbance of the reactive medium involving the unimolecular
147 phototransformation of an initial species *A*, into its photoproduct (*B*) is given by the
148 logarithmic Eq.1.¹⁶

149 Eq.1 has been established for a homogeneously and continuously stirred solution, which is
 150 subjected to a monochromatic, non-isosbestic and continuous irradiation (λ_{irr}) at constant
 151 temperature. Also, it is assumed that the concentration of the excited-state species is
 152 negligible and at the irradiation wavelength (λ_{irr}) species *A* and *B* may absorb different
 153 amounts of light ($P_{\lambda_{irr}}$), i.e. the absorption coefficients of the species may be different ($\epsilon_A^{\lambda_{irr}} \neq$
 154 $\epsilon_B^{\lambda_{irr}} \neq 0$). For the present study, the species *A* and *B* correspond to dacarbazine, *DBZ*, and its
 155 photoproduct, *PP*. (The photo product's chemical structure has not been identified with
 156 certainty).

$$\begin{aligned}
 A_{tot}^{\lambda_{irr}/\lambda_{obs}}(t) = & A_{PP}^{\lambda_{irr}/\lambda_{obs}}(\infty) + \frac{A_{DBZ}^{\lambda_{irr}/\lambda_{obs}}(0) - A_{PP}^{\lambda_{irr}/\lambda_{obs}}(\infty)}{A_{DBZ}^{\lambda_{irr}/\lambda_{irr}}(0) - A_{PP}^{\lambda_{irr}/\lambda_{irr}}(\infty)} \times \frac{l_{\lambda_{obs}}}{l_{\lambda_{irr}}} \\
 & \times \text{Log} \left[1 + \left(10^{-\left[\left(A_{DBZ}^{\lambda_{irr}/\lambda_{irr}}(0) - A_{PP}^{\lambda_{irr}/\lambda_{irr}}(\infty) \right) \times \frac{l_{\lambda_{irr}}}{l_{\lambda_{obs}}} \right]} - 1 \right) \right. \\
 & \left. \times e^{k_{DBZ}^{\lambda_{irr}} \times t} \right] \tag{1}
 \end{aligned}$$

157
 158 where $l_{\lambda_{irr}}$ represents the optical path length of the irradiation beam inside the sample and
 159 $l_{\lambda_{obs}}$ is the optical path length of the spectrophotometer monitoring light. The absorbances
 160 (A^{λ} / λ) in Eq.1 correspond to the actual measurements by the instrument (i.e. along $l_{\lambda_{obs}}$)
 161 performed on the reactive medium, at a given reaction time ($A_{tot}^{\lambda_{irr}/\lambda_{obs}}(t)$), at the initial time
 162 ($t=0, A_{DBZ}^{\lambda_{irr}/\lambda_{obs}}(0)$), and at the end of the reaction ($t = \infty, A_{PP}^{\lambda_{irr}/\lambda_{obs}}(\infty)$ where only the
 163 photoproduct is present). The absorbances vs. time (the traces) can be read out from the
 164 spectra at the particular wavelengths of irradiation (λ_{irr}) and observation (λ_{obs}) which might or

165 not be the same. Therefore, each kinetic profile is dually labelled by the irradiation and the
 166 observation wavelengths ($\lambda_{irr}/\lambda_{irr}$ or $\lambda_{irr}/\lambda_{obs}$).

167

168 The exponential factor in Eq.1, $k_{DBZ}^{\lambda_{irr}}$, representing the overall photoreaction rate-constant, is
 169 analytically expressed by

170

$$171 \quad k_{DBZ}^{\lambda_{irr}} = \Phi_{DBZ \rightarrow PP}^{\lambda_{irr}} \times \varepsilon_{DBZ}^{\lambda_{irr}} \times I_{\lambda_{irr}} \times F_{\infty}^{\lambda_{irr}} \times P_{\lambda_{irr}} = \beta_{\lambda_{irr}} \times P_{\lambda_{irr}} \quad (2)$$

172

173 where $\Phi_{DBZ \rightarrow PP}^{\lambda_{irr}}$ is the forward quantum yield of DBZ photodegradation, realised at the non-
 174 isosbestic irradiation wavelength (λ_{irr}), $\varepsilon_{DBZ}^{\lambda_{irr}}$ is the molar absorption coefficient of DBZ, $P_{\lambda_{irr}}$ is
 175 the radiant power, and $F_{\infty}^{\lambda_{irr}}$ the photokinetic factor expressed as

176

$$F_{\infty}^{\lambda_{irr}} = \frac{1 - 10^{-\left(A_{tot}^{\lambda_{irr}/\lambda_{irr}(\infty)} \times \frac{I_{\lambda_{irr}}}{I_{\lambda_{obs}}} \right)}}{A_{tot}^{\lambda_{irr}/\lambda_{irr}(\infty)} \times \frac{I_{\lambda_{irr}}}{I_{\lambda_{obs}}}} \quad (3)$$

177 The set of Eqs.1–3, are also applicable for the case where only species A absorbs as the
 178 corresponding equations can be retrieved from Eqs.1–3 by considering the quantities relative
 179 to the photoproduct equal to zero (i.e. $A_{tot}^{\lambda_{irr}/\lambda_{irr}(\infty)} = A_{PP}^{\lambda_{irr}/\lambda_{obs}(\infty)} = \varepsilon_{PP}^{\lambda_{irr}} = 0$).

180

181 Nevertheless, the application of Eqs.1–3 to the case where both species (A and B) absorb the
182 excitation light was conditional to $F_{\infty}^{\lambda_{irr}}$ being higher than 1.2 ($A_{PP}^{\lambda_{irr}}/\lambda_{irr}(\infty) < 0.65$). This has
183 proven to be a simple limitation as the former condition can easily be met by lowering the
184 concentration of the initial species or possibly by reducing the path length of the irradiation
185 ($l_{\lambda_{irr}}$).

186

187 The AB(1 Φ) photodegradation reactions that are well described by Eq.1 are considered to obey
188 Φ –order kinetics.

189

190 Since the differential equations of thermal and photochemical reactions are different, it is
191 expected that the mathematical formulae of their respective integrated rate-law equations be
192 different, and therefore a specific order for each reaction should, as a consequence, be
193 established. This statement holds equally for the case where two different thermal reactions
194 are considered (e.g., zeroth– and first–order reactions) as well as for reactions of different
195 nature (photochemical and thermal reactions). As a matter of fact, Φ –order kinetics would be
196 ill-described by for instance 1st–order kinetics (as it would be if either 0th or 2nd order kinetics
197 were used). From this point of view, the photodegradation kinetics of drugs should be better
198 described by Φ –order kinetics instead of the usually employed treatments that correspond to
199 thermal reactions. A comprehensive discussion of the properties Φ –order kinetics and its
200 flexibility compared to thermal reaction orders has been previously provided.¹⁶

201 Also, the Φ –order kinetics presents the advantage of providing the absolute values of the
202 quantum yield (and/or the $\beta_{\lambda_{irr}}$ factors) irrespective of the radiant power used (as set out in

203 Eq.2). It therefore provides a plausible tool to perform high concentration/light radiant flux
204 tests such as those recommended by ICH.

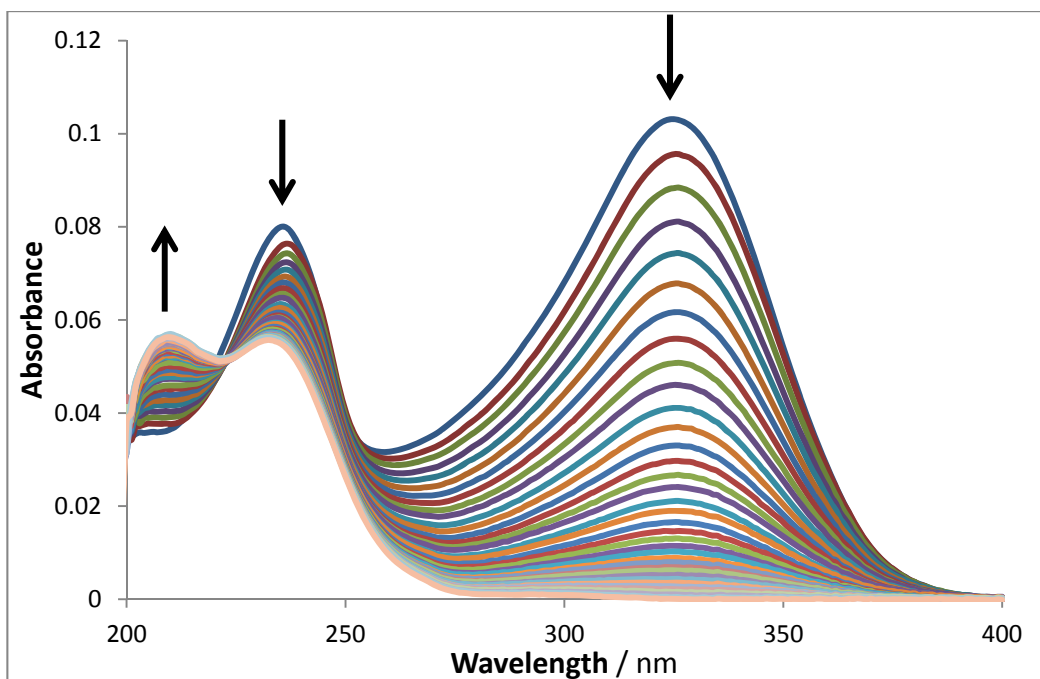
205

206 **3.2. DBZ Photodegradation in ethanol**

207 In ethanol, the absorption spectrum of *DBZ* in the dark is characterised by two main and broad
208 absorption 200–250 and 280–400 nm regions, spanning the UVB, UVA and a small section of
209 the visible spectral ranges (Fig. 1). The maxima for *DBZ* are located at 235 and 325 nm, with the
210 latter much broader and higher in intensity than the former. The long-wavelength absorption
211 band is probably due to the $\pi \rightarrow \pi^*$ transitions occurring in the extended double bond system
212 formed between the ring and its adjacent unsaturated azo-group (Scheme 1). It could also be
213 suggested that this band might correspond to a charge-transfer (CT) transition. In the case of
214 such an interpretation, the intramolecular CT transitions might be attributed to a resonance
215 interaction involving $n \rightarrow \pi$ conjugation. Since the π^* orbital is situated on the double bond
216 system then the effect of the transition is to transfer a charge from the electron-donating
217 substituent (e.g. $-\text{N}(\text{CH}_3)_2$) to the electron accepting group (e.g. pyrazole ring).^{20,21}

218

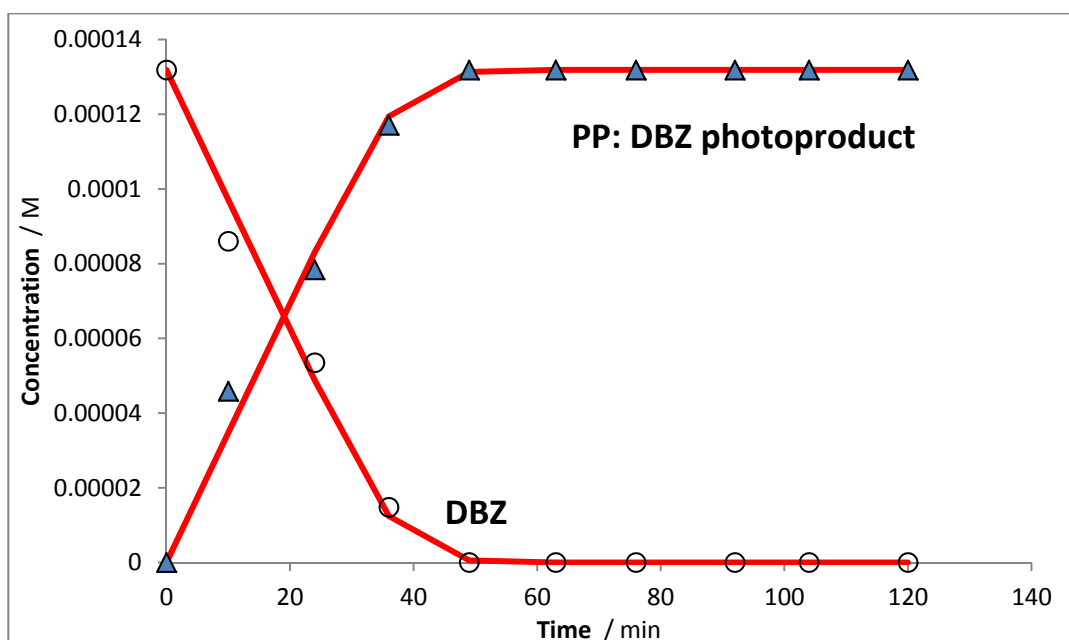
219 A number of spectral changes occur when subjecting the reactive medium to monochromatic
220 irradiation, including the gradual decrease of both peaks, with a complete disappearance of the
221 long-wavelength band at the end of the reaction. During the reaction progress a new peak
222 emerges at *ca.* 206 nm. This behaviour is observed irrespective of the wavelength of the
223 irradiation beam. Such features indicate a significant disturbance of the π system, and overall,



224

225 **Figure 1:** Evolution of the electronic absorption spectra of 5.47×10^{-6} M Dacarbazine (*DBZ*) in
 226 ethanol, when irradiated continuously with a monochromatic beam at 325-nm (total irradiation
 227 time 1500 s at a radiant power of $P_{325} = 1.84 \times 10^{-6}$ einstein. $s^{-1} \cdot dm^{-3}$). The arrows indicate the
 228 direction of the evolution of the absorption bands during the photoreaction.

229



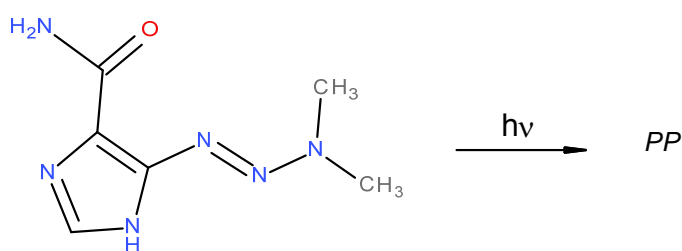
230

231 **Fig 2:** Evolution of *DBZ* concentration ($C_{DBZ}(0) = 1.32 \times 10^{-4}$ M) over the photodegradation time
 232 and the simultaneous formation of the photoproduct. The reaction medium was monitored by
 233 HPLC while irradiated continuously with a monochromatic beam at 325 nm ($P_{325} = 1.02 \times 10^{-6}$
 234 einstein $s^{-1} dm^{-3}$). Circles and triangles: experimental data; Lines: fitting of the data with Eq.1.

235 clearly point out to a chemical change due to irradiation. It is worth noting that *DBZ* is stable in
236 the dark with no recorded variation of its spectrum over a long time.

237

238 The chromatograms obtained by monitoring the reaction medium by HPLC showed the
239 presence of only two peaks attributable to *DBZ* and its photoproduct, *PP* (as laid out in Scheme
240 1). The concentration of *DBZ* decreased continuously with irradiation time until reaching a zero
241 value while that of *PP* increased (Fig.2). The good fit of the experimental data with Eq.1 (with
242 the same rate-constant for both species) corroborates the occurrence of a unimolecular
243 mechanism of the AB(1Φ) type (Scheme 1).



244

245 **Scheme 1.** Proposed photodegradation reaction of *DBZ* in ethanol.

246

247

248

249 **3.3. Photodegradation kinetics of *DBZ***

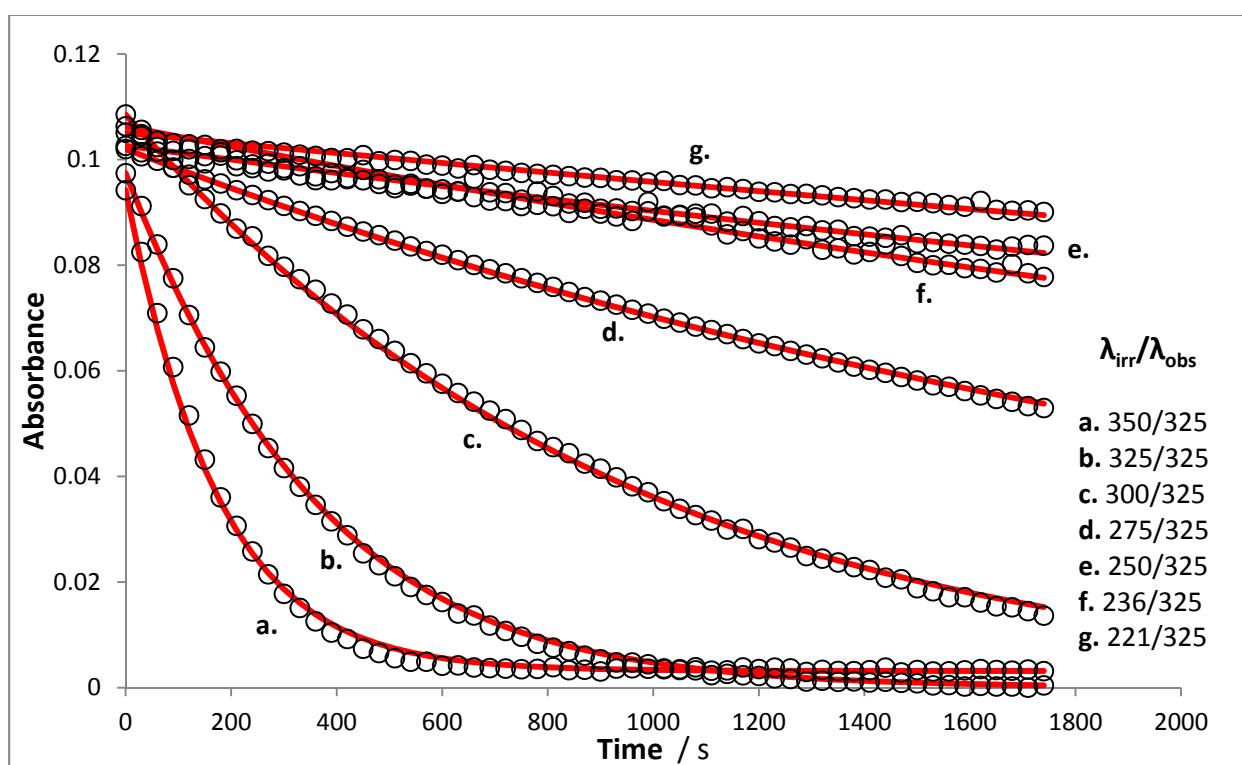
250

251 The investigation of *DBZ* kinetics was performed on freshly prepared and equally concentrated
252 solutions subjected to a series of irradiations whose beams' wavelengths (λ_{irr} = 350, 325, 300,
253 275, 250, 236 and 221 nm) covered almost entirely the absorption spectrum of the drug.

254 The kinetic traces were collected by observing the timely variation of the absorbance of the
 255 reactive medium at a unique observation wavelength ($\lambda_{obs} = 325$ nm) for each experiment
 256 performed at a given irradiation wavelength (Fig. 3). These traces are labelled by their
 257 irradiation/observation wavelengths ($\lambda_{irr}/\lambda_{obs}$).

258

259



260

261 **Fig. 3:** Photokinetic profiles of *DBZ* in ethanol (5.47×10^{-6} M) obtained at different irradiation
 262 wavelengths ($\lambda_{irr} = 350, 325, 300, 275, 250, 236$ and 221 nm) and observed at $\lambda_{obs} = 325$ nm.
 263 The circles represent experimental data whereas the solid lines represent the fitting of the
 264 traces with Eq.1.

265

266

267 The subsequent good fitting of these traces with Eq.1 further confirmed that *DBZ* obeyed a
268 unimolecular phototransformation which was well described by Φ -order kinetics. This also
269 underlines the usefulness of the model equation (Eq.1) in depicting AB(1 Φ) photoreactions
270 kinetics at any non-isosbestic and monochromatic irradiation.

271
272 The kinetic studies on *DBZ* are very scarce. As far as we are aware, no data is available on *DBZ*
273 photodegradation in organic media. In water solution, *DBZ* degradation under polychromatic
274 fluorescent light was reported to obey apparent first-order kinetics even though the data
275 presented showed a good linear correlation between the remaining *DBZ* concentration (in
276 percentage) with reaction time.⁹ Similar treatment of the kinetic data are predominant in
277 photodegradation studies.¹² However, owing to the fact that the 0th-, 1st-, and 2nd-order
278 kinetic classical models were basically developed for thermal reaction, they should not in
279 principal be applicable to photodegradation data due to the differences found in the
280 differential equations of thermal and photochemical reactions. It is also worth noting that
281 there are many examples where the same experimental data of a given drug photoreaction
282 could be fitted with equations corresponding to two different classical reaction-orders,¹²
283 hence, raising some serious issues about the applicability of the aforementioned approach.¹⁶
284 This situation does not seem to be specific to AB(1 Φ) reactions.^{12,13} In this respect, the Φ -order
285 kinetics seems to be a viable and more precise alternative to the classical treatments.

286
287 The analysis of Fig.3 suggests that *DBZ* photodegradation increases with irradiation
288 wavelength, with the fastest reactions observed for $\lambda_{irr} > 300$ nm. However, a definite
289 conclusion on the basis of this observation might be dubious as the formula of the
290 photodegradation rate-constant, involves a contribution of reaction attributes, reactants'

291 parameters and some experimental conditions whose values might considerably differ
292 between wavelengths (e.g. the absorption coefficients, the radiant power...etc). Therefore, it is
293 not reliable to directly compare the overall rate–constant values. In a more consistent strategy,
294 the evaluation of all the reaction parameters is needed. For instance, the determination of the
295 photochemical quantum yield values and their possible variation with irradiation would shed
296 light on the efficiency of the photodegradation as well as on their contribution to the rate–
297 constant value.

298

299 **3.4. DBZ photochemical quantum yields**

300 The fitting of the experimental kinetic profiles of *DBZ* photodegradation to Eq.1 (Fig.3) allows
301 the extraction of the overall rate–constant values for each individual experiment. These values
302 together with the analytical expression of $k_{DBZ}^{\lambda_{irr}}$ (Eq. 2) are used to work out the values of *DBZ*
303 quantum yield values under any monochromatic irradiation condition (Table 1).

304

305 The efficiency of *DBZ* photodegradation is wavelength–dependent with a significant 50–fold
306 increase between 235 and 350 nm. Its highest values ($\Phi_{DBZ \rightarrow PP}^{\lambda_{irr}} > 0.015$) were recorded for
307 wavelengths higher than 300 nm, which indicates that the lowest excited state produced from
308 the long-wavelength transition plays a major role in the photodegradation of the anti–cancer
309 drug.

310

311 The phenomenological trend of the experimental data relative to our *DBZ* photodegradation
312 quantum yields in ethanol is well reproduced by a sigmoidal pattern with respect to the

313 variation of the irradiation wavelength (Fig. 4). Even though the plateau region of the sigmoid
314 was not reached for DBZ, the general pattern is consistent with the data observed for other
315 drugs.^{16,18,22-24} The sigmoid function, given by Eq.4, yields values for $\Phi_{DBZ \rightarrow PP}^{\lambda_{irr}}$ which agree well
316 with their experimental counterparts listed in Table 1. The two sets of values are linearly
317 correlated as indicated by the inset of Fig.4. In this respect, Eq.4 can be used to predict the
318 quantum yield absolute values at any irradiation wavelength between 220 and 350 nm.

319

$$320 \quad \Phi_{DBZ \rightarrow PP}^{\lambda_{irr}} = \frac{0.263}{1 + 399 \times e^{-0.0265 \times (\lambda_{irr} - 180)}} \quad (4)$$

321

322 The acute evolution of the quantum yield values over the 150–nm spectral range, clearly
323 indicate that monochromatic light is the best tool to characterise the photoreactivity of drugs.
324 Incidentally, such a result on quantum yields cannot be achieved using the classical thermal
325 kinetic models. This also points out the challenge of obtaining reliable measurements of
326 reaction quantum yields when using polychromatic and pseudo–monochromatic lights (the
327 latter are most often obtained as filtered light from lamps whose beams’ bandwidths may vary
328 from a few tens to more than a hundred nanometres).²⁵ The results obtained from such
329 measurements for the evaluation of quantum yield values can only be considered as
330 approximations as they ought to provide only average values.

331

332 Even though no quantum yield values are available in the literature for *DBZ*, the results of this
333 study can be compared to those obtained for other drugs since, conversely to the reaction
334 rate–constants, the photochemical photodegradation quantum yields are absolute parameters.

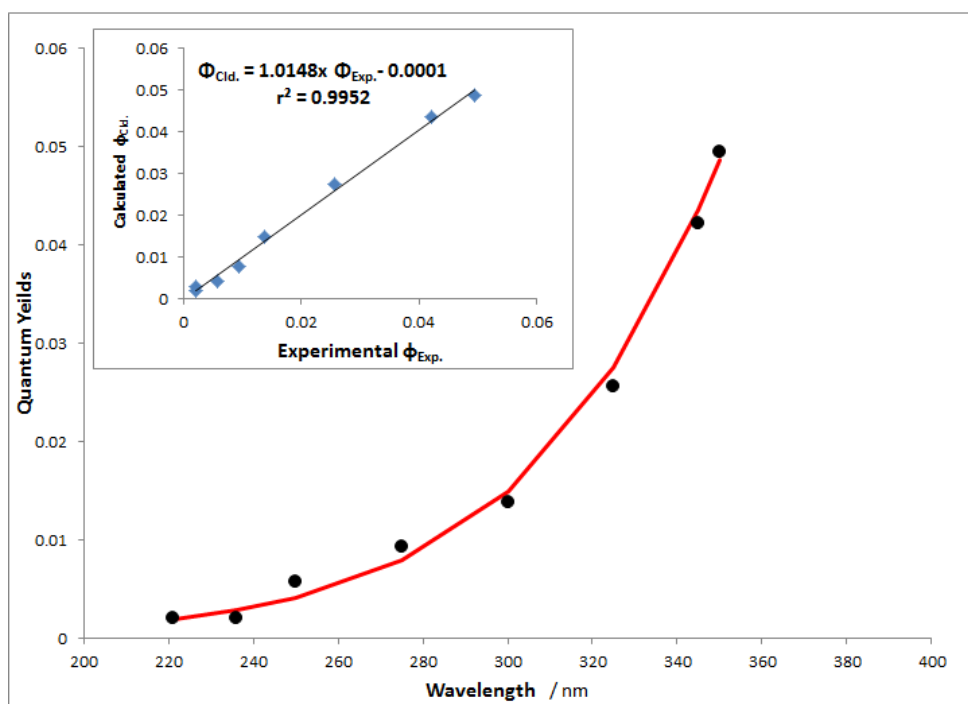
335 **Table 1**

336 Quantum yields, overall rate-constants, absorption coefficient and radiant power values for
 337 DBZ photodegradation reactions under various monochromatic irradiation wavelengths.

λ_{irr}	$\epsilon_{DBZ}^{irr} / M^{-1}.cm^{-1}$	$P_{\lambda irr} / \text{einstein s}^{-1}dm^{-3}$	$k_{DBZ}^{\lambda irr} \times 10^3 / s^{-1}$	$\Phi_{DBZ \rightarrow PP}^{\lambda irr}$
350	9896	2.99×10^{-6}	6.63	$(49 \pm 1.11) \times 10^{-3}$
345	12580	2.17×10^{-6}	5.55	$(42 \pm 1.65) \times 10^{-3}$
325	18864	2.16×10^{-6}	4.17	$(23 \pm 5.84) \times 10^{-3}$
300	12469	1.45×10^{-6}	1.37	$(16 \pm 3.31) \times 10^{-3}$
275	7068	1.44×10^{-6}	0.45	$(9 \pm 1.80) \times 10^{-3}$
250	7157	1.26×10^{-6}	0.23	$(4 \pm 2.81) \times 10^{-3}$
236	14639	1.49×10^{-6}	0.20	$(1 \pm 1.00) \times 10^{-3}$
221	9476	1.53×10^{-6}	0.13	$(1 \pm 1.00) \times 10^{-3}$

338

339



340

341 **Fig. 4:** Average forward $\Phi_{DBZ \rightarrow PP}^{\lambda irr}$ (filled circles) quantum yields calculated for irradiation
 342 wavelengths $\lambda_{irr} = 350, 345, 325, 300, 275, 250, 236$ and 221 nm. The line represents the
 343 fitting of the data with Eq.7. Inset: Calculated (Eq.4), $\Phi_{Cld.}$, vs. experimental, $\Phi_{Exp.}$, values of
 344 photochemical quantum yields (Table1).

345 Our results for *DBZ* ($\Phi_{DBZ \rightarrow PP}^{\lambda_{irr}}$) are about 10-fold lower than those obtained for nifedipine, a
346 very light sensitive cardiovascular drug, which obeys AB(1 Φ) Φ -order kinetics,¹⁶ and 2-5 times
347 lower than those obtained for *trans*-Montelukast, a photoreversible AB(2 Φ) system.¹⁸
348 However, for all these drugs, the quantum yield values increased with the irradiation
349 wavelength and their photochemical efficiencies were the smallest for the shortest wavelength
350 transitions (mostly below 270 nm). Obviously, our findings do not corroborate the affirmation,
351 concerning the quantum yield dependency with irradiation wavelength, stating that "*the*
352 *quantum yield is a wavelength independent quantity and thus can be determined at any*
353 *wavelength that the substance absorbs, although a greater precision can be gained near the*
354 *absorption maximum*".¹³ Therefore, our results recommend that the photodegradation
355 reaction quantum yields of drugs should be determined experimentally to confirm whether or
356 not they are wavelength-dependent.

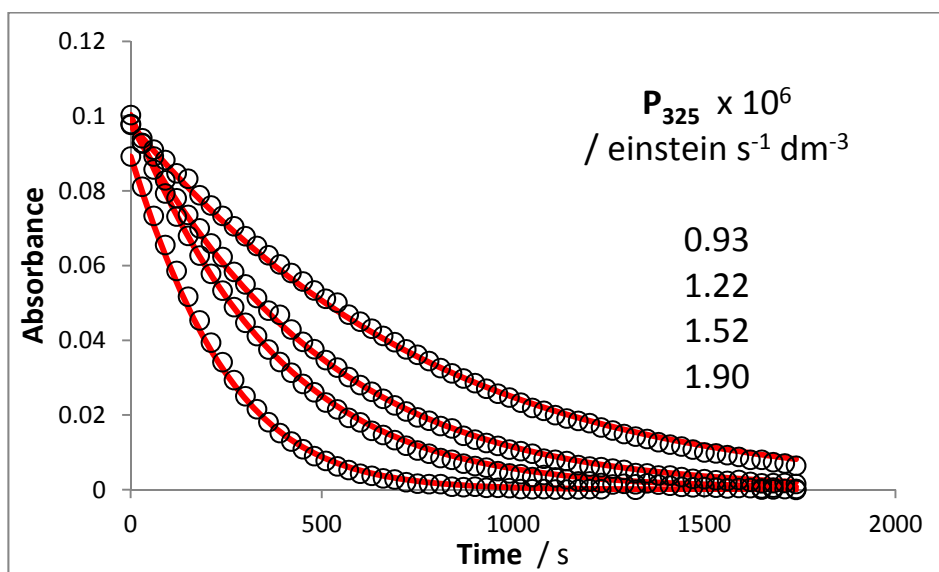
357

358 **3.5. DBZ-actinometer**

359 Drugs are not usually used as actinometers and no kinetic-based methods for actinometry
360 have so far been reported.^{12,13,25,26} In previous studies it has been shown that drugs and
361 chemical systems which are well described by Φ -order kinetics may be exploited as
362 actinometers.^{15,16,18} Indeed, the Φ -order equations are flexible enough to bring forward the
363 potential and facilitate the development of new drug-actinometers based on the kinetic data
364 of their photodegradations. In the context of pharmaceuticals, proposing new actinometers is
365 important since the one recommended by ICH,²⁷ namely the quinine hydrochloride
366 actinometer, presents various drawbacks that seriously hamper its application to
367 photostability testing purposes.²⁸⁻³¹

368

369

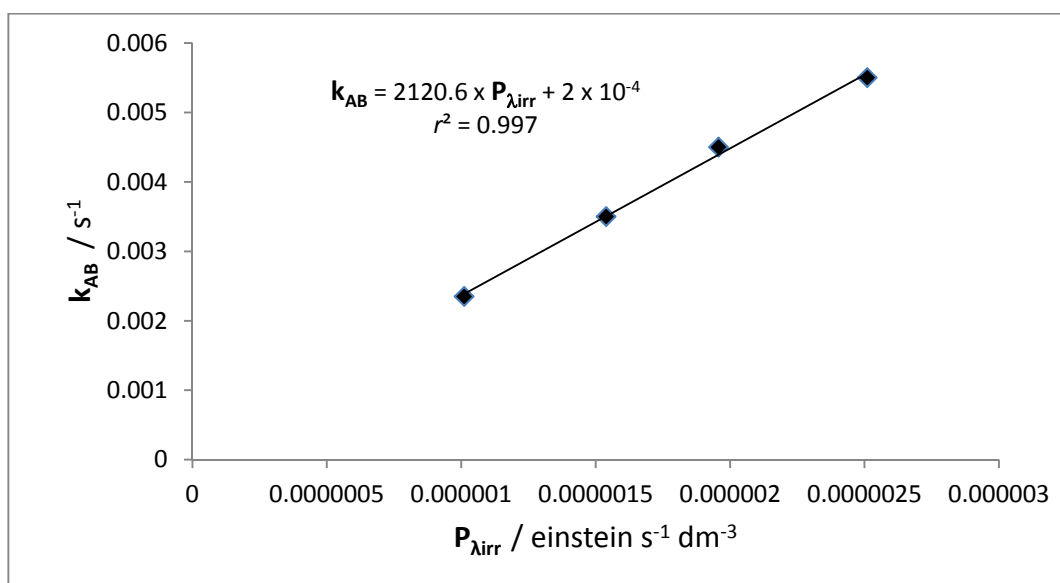


370

371 **Fig. 5:** Effect of increasing the radiant power, P_{325} , of a 325-nm monochromatic irradiation
372 beam on the kinetic traces of DBZ (5.47×10^{-6} M). Circles represent experimental data ($\lambda_{obs} =$
373 325 nm) and the solid lines correspond to the best fit traces to Eq.1.

374

375



376

377 **Fig. 6:** An example of a linear correlation between of the k_{DBZ}^{350} parameter of the traces against
378 the radiant power, P_{350} for DBZ in ethanol.

379

380 Testing the potential of DBZ for actinometry was performed within the 270-350 nm spectral
381 range where *DBZ* is most photoactive (Table 1). Five irradiation wavelengths ($\lambda_{irr} = 350, 345,$
382 $325, 300,$ and 275 nm) were selected for the study. A series of freshly prepared *DBZ* solutions
383 were each irradiated at one of the selected wavelengths with a series of different radiant
384 powers of the excitation beam ($P_{\lambda_{irr}}$, spanning the capacity of our instrumentation). The traces
385 for *DBZ* photodegradations were collected while monitoring the medium at the maximum
386 intensity of *DBZ* absorption spectrum ($\lambda_{obs} = 325$ nm). These traces have then been fitted to
387 Eq.1 (Fig.5), and the respective values of the rate-constants ($k_{DBZ}^{\lambda_{irr}}$) determined.

388

389 According to Eq.2, the higher the $P_{\lambda_{irr}}$ values the faster the photodegradation (i.e. the higher
390 the $k_{DBZ}^{\lambda_{irr}}$ values). Also, as predicted by the latter equation, $k_{DBZ}^{\lambda_{irr}}$ and $P_{\lambda_{irr}}$ values were found to
391 linearly correlate with very small intercepts (close to zero values) and almost unitary
392 correlation coefficients (Fig.6 and Table 2).

393

394 For the selected irradiation wavelengths, the gradients of these equations, expressed here as
395 the factors $\beta_{\lambda_{irr}}$ (Eq.2), produce a triangular correlation with the irradiation wavelength. This
396 correlation can readily be represented by two linear relationships as given in Fig.7 (with
397 correlation coefficients exceeding 0.99). Using the linear relationships, allows predicting the
398 values of $\beta_{\lambda_{irr}}$ for any irradiation wavelength situated between 275 and 350 nm. But more
399 importantly, such $\beta_{\lambda_{irr}}$ values effectively serve the determination of the radiant power of an
400 unknown, though monochromatic, light source within the aforementioned range through a
401 rearranged Eq.3, as

402 **Table 4:** Correlation equations for the variation of DBZ photodegradation overall rate-
 403 constants ($k_{NIS}^{\lambda_{irr}}$) with radiant power ($P_{\lambda_{irr}}$), the corresponding $\beta_{\lambda_{irr}}$ factors, and the span of
 404 radiant power employed for various monochromatic irradiations.

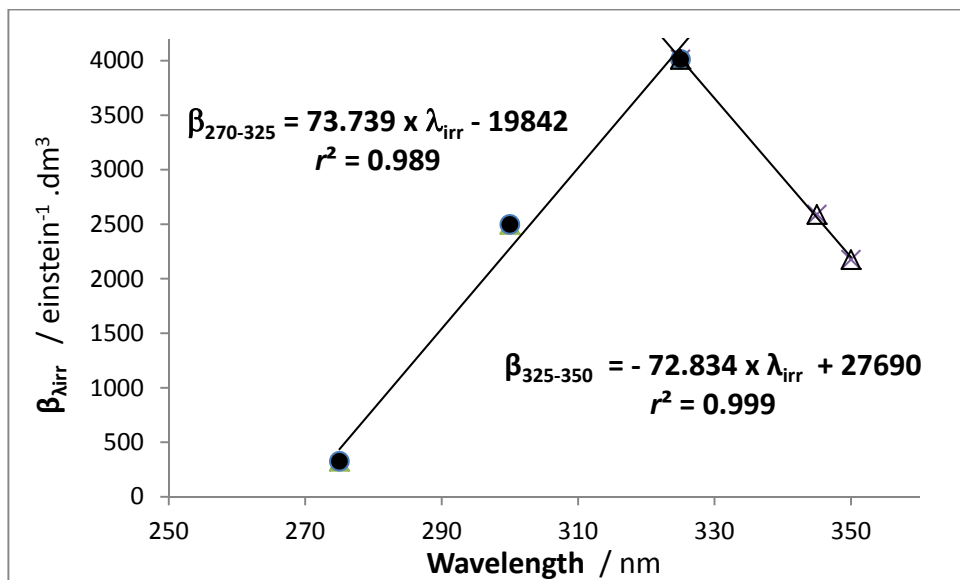
Irradiation wavelength λ_{irr} / nm	Equation of the line ^a $k_{DBZ}^{\lambda_{irr}} = \beta_{\lambda_{irr}} \times P_{\lambda_{irr}} + \text{intercept}$	Correlation coefficient, r^2	$P_{\lambda_{irr}} \times 10^7$ / einst.s ⁻¹ .dm ⁻³
350	$2120.6 \times P_{350} + 0.0002$	0.9969	1.01 – 2.51
345	$2589.8 \times P_{345} - 0.0003$	0.9830	0.95 – 2.20
325	$4013.2 \times P_{300} - 0.0024$	0.9499	0.93 – 1.90
300	$2499.3 \times P_{300} - 0.0017$	0.9987	1.05 – 1.31
275	$326.26 \times P_{275} - 0.0001$	0.9991	0.78 – 1.64

405 ^a $k_{NIS}^{\lambda_{irr}}$ and intercepts expressed in s⁻¹ and $\beta_{\lambda_{irr}}$ in einstein⁻¹.dm³.

406

407

408



409

410 **Fig.7:** Correlations of $\beta_{\lambda_{irr}}$ with irradiation wavelength. $\beta_{\lambda_{irr}}$ is expressed in einstein⁻¹ dm⁻³

411

412
$$P_{\lambda_{irr}} = \frac{k_{DBZ}^{\lambda_{irr}}}{\beta_{\lambda_{irr}}} \quad (5)$$

413

414 Therefore, *DBZ* can act as an actinometer for that range of wavelengths by simply applying the
415 following actinometric procedure: (i)– subject a freshly prepared (*ca.* 5×10^{-6} M) solution of the
416 drug *DBZ* in ethanol to the monochromatic light (between 275 and 350 nm) of the unknown
417 source, (ii)– collect its full kinetic trace by monitoring the variation of the absorbance at 325 nm
418 ($\lambda_{irr}/325$), (iii)– fit it with Eq.1 and determine its $k_{DBZ}^{\lambda_{irr}}$, (iv)– determine the value of the $\beta_{\lambda_{irr}}$
419 factor from the linear relationships (Fig. 7) and finally (iv)– work out the value of the unknown
420 light source radiant power ($P_{\lambda_{irr}}$) from Eq.5.

421

422 It is interesting to notice that in general, the variation of $\beta_{\lambda_{irr}}$ with λ_{irr} will depend on the
423 various parameters making up the general expression of the $\beta_{\lambda_{irr}}$ factors (Eq.2). However, the
424 obtained $\beta_{\lambda_{irr}}$ values for a given actinometer can be used for the determination of $P_{\lambda_{irr}}$
425 irrespective of how $\beta_{\lambda_{irr}}$ particularly correlate with λ_{irr} . A triangular pattern has been found
426 here for *DBZ*, but linear relationships were obtained for Nifedipine,¹⁶ Montelukast¹⁸ and a
427 diarylethene derivative, *DAE*.¹⁵

428

429 Furthermore, it is reasonable to envisage that a combination–actinometer, involving several
430 individual drugs and chemical compounds can be proposed with the aim to cover a larger
431 dynamic range (e.g. *DBZ* for 275–350 nm and *DAE* for 400–580 nm ranges).

432

433 The present actinometric overall approach has the double advantage of using kinetic data that
434 are easily collected and avoiding the usual problems encountered for other actinometers. In
435 addition of being simple-to-implement, it can be run without depending on the knowledge of
436 the reaction attributes (as the quantum yields) as long as the system employed obeys a
437 unimolecular AB(1Φ) kinetics. This approach might prove to be useful for the development of
438 other drug-actinometers.

439
440 If our actinometric method can certainly be applied to situations where high radiant power is
441 used for drugs absorbing below 350 nm, it can however only be used for monochromatic
442 irradiation beams. This might be seen as a limitation for applications using polychromatic light.
443 It is though important to stress the fact that integrated rate-laws of such a polychromatic
444 absorption have not yet been made available. The actual actinometers used for that purpose
445 present important limitations that shed doubt on their reliability. It is in our opinion a serious
446 issue that ought to be acknowledged and addressed in order to contribute to the improvement
447 of photostability and/or photosafety testing.

448
449 It is also important to notice that the $\beta_{\lambda_{irr}}$ factors (Eq.2), labelled lately the *pseudo-rate-*
450 *constants*,²³ offer an undeniable advantage of rendering possible the direct comparison of
451 reactivity for different photodegradation reactions performed in the same solvent but
452 irrespective of the molecule and experimental conditions used. Indeed, the pseudo-rate-
453 constants of the group of active pharmaceutical ingredients reported in Table 5, indicate that
454 Montelukast has the highest $\beta_{\lambda_{irr}}$ value and hence, in the optimal conditions, is the most
455 reactive drug of the series (if the absorption spectra of the molecules, i.e. the irradiation

456 wavelengths involved, are overlooked). From this point of view, Montelukast photodegrades
457 faster than Nisoldipine, a cardiovascular drug similar to Nifedipine, that is considered one of
458 the fastest known photoreactive drugs. This is a significant result as for these two molecules
459 the maximal values of $\beta_{\lambda_{irr}}$ are recorded at relatively close irradiation wavelengths of 360 and
460 370 nm for Montelukast and Nisoldipine, respectively. In this context, DBZ has moderate
461 photodegradation reactivity amongst the series studied (recording *ca.* half the $\beta_{\lambda_{irr}}$ factor of
462 Nisoldipine).

463

464 As a matter of fact, since the pseudo-rate-constants of drugs depend on many factors (Eq.2), it
465 is not possible to find a simple correlation of their values with those of the corresponding
466 quantum yields (Table 5). For instance, the maximum experimental value of the quantum yield
467 of Fluvoxamine is 2.4-folds higher than that of Montelukast but the maximum value of the $\beta_{\lambda_{irr}}$
468 factor of the latter is 13.5 times that of the former. This is therefore a compelling example
469 demonstrating that a comparison of quantum yields would not be informative on
470 photoreactivity of transforming molecules in solution (such a comparison might eventually be
471 considered for AB(1 Φ) systems where only the initial species absorbs the irradiation light if the
472 absorption coefficients of the compared systems do not show important differences at λ_{irr} ,
473 such as for DBZ in the range 300-400 nm). These findings might help with the difficulty of
474 comparing photodegradation studies, as has been reported in the pharmaceutical
475 literature,^{12,13} and emphasises further a strong advice against using the thermal 0th-, 1st- and/or
476 2nd order kinetic treatments that are usually employed in dealing with data of
477 photodegradation reactions of drugs.

478

479 **Table 5:** Comparative ranges of photodegradation wavelengths (λ_{irr}), quantum yields (Φ) and
 480 pseudo-rate-constants ($\beta_{\lambda_{irr}}$) for a series of pharmaceutical drugs.

Drugs ^a	Wavelength ^b /nm	Quantum yield	Pseudo-rate-constant ^c	Ref.
E-Montelukast	258 – 360	0.065 – 0.180	2251 – 28069	18
Nisoldipine	320 – 390	0.304 – 0.351	7558 – 8851	24
Dacarbazine	300 – 350	0.016 – 0.049	2121 – 4013	-
E-Sunitinib	340 – 480	0.020 – 0.026	1560 – 5847	22
E-Fluvoxamine	260 – 290	0.013 – 0.435	818 – 2077	23

481 ^a : measurements performed in ethanol for drugs' concentration varying between 1.8×10^{-6} and
 482 8.9×10^{-6} M.

483 ^b : wavelength domain of the photodegradation causative range (which includes the long
 484 wavelength peak of maximum absorption).

485 ^c : $\beta_{\lambda_{irr}}$ factors expressed in $\text{einstein}^{-1} \text{dm}^3$.

486

487

488

489 **4. Conclusion**

490

491 The photodegradation of *DBZ* in ethanol proceeds through a unimolecular reaction leading to
 492 the formation of a single photoproduct. The reaction progress with time has been proven to
 493 obey Φ -order kinetics. The *DBZ* photodegradation quantum yields, determined in the region
 494 221–350 nm, are wavelength dependent and their variation has been modelled by a sigmoid
 495 function. Their absolute values are relatively low ($\Phi_{DBZ \rightarrow PP}^{\lambda_{irr}} < 5 \times 10^{-2}$) but a rather large, 50-
 496 fold, increase of the quantum yield has been found between the UVB and UVA excitations. The

497 UVA region of the *DBZ* spectrum (with $\Phi_{DBZ \rightarrow PP}^{\lambda_{irr}} > 0.01$) represents the main photodegradation
498 causative range.

499

500 The Φ -order kinetic equations have also been used to develop a *DBZ*-actinometric procedure
501 that makes this anti-cancer drug a functional actinometer in the 275–350 nm range. The
502 procedure proposed here should work well for monochromatic irradiation. However, both the
503 sigmoid variation of $\Phi_{DBZ \rightarrow PP}^{\lambda_{irr}}$ and the triangular shape of the $\beta_{\lambda_{irr}}$ factor indicate that *DBZ*-
504 actinometry is most likely not suitable for polychromatic light beams. In fact, this might be the
505 case for many actinometers since their individual quantum yield values should *a priori* be
506 considered wavelength dependent as should their $\beta_{\lambda_{irr}}$ factors. In this respect, the radiant
507 power values that are generally reported for polychromatic light sources must be considered
508 with caution as they might correspond to averages rather than absolute values.

509

510 The Φ -order kinetic equations prove to be much useful tools for the characterization and
511 quantification of photodegradation of AB(1 Φ) drug systems which in addition offer flexibility to
512 develop new and reliable drug-actinometers.

513 **References**

- 514 1 Bonifazi E, Angelini G, Meneghini CL 1981. Adverse Photo Reaction to Dacarbazine (DTIC).
515 Contact Dermatitis, 7(3):161.
- 516 2 Nussbaumer S, Bonnabry P, Veuthey J, Fleury-Souverain S 2011. Analysis of anticancer
517 drugs: A review. *Talanta*, 85:2265-2289.
- 518 3 Tsuji T, Ohtsubo T, Umeyama T, Sudou M, Komesu K, Matsumoto M, Yoshida Y, Banno R,
519 Mikami T, Kohno T 2014. Methods for reducing Dacarbazine photodegradation and its
520 accompanying venous pain. *Yakugaku Zasshi*. 134(9), 981-986.
- 521 4 Asahi M, Matsushita R, Kawahara M, Ishida T, Emoto C, Suzuki, N, Kataoka O, Mukai C,
522 Hanaoka M, Ishizaki J, Yokogawa K, Miyamoto K 2002. Causative agent of vascular pain
523 among photodegradation products of dacarbazine. *Journal of Pharmacy and*
524 *Pharmacology*, 54(8):1117-22.
- 525 5 Avendaño C, Menéndez JC 2008. *Medicinal Chemistry of Anticancer Drugs*, Elsevier,
526 Amsterdam.
- 527 6 Shealy YF, Krauth CA, Montgomery JA 1962. Imidazoles. I. Coupling reactions of 5-
528 diazoimidazole-4-carboxamide. *Journal of Organic Chemistry*, 27:2150-2154.
- 529 7 Horton JK, Stevens MFG 1981. Triazines and Related Products. Part 23. New Photo-
530 products from 5-Diazoimidazole-4-carboxamide (Diazo-IC). *Journal of the Chemical Society*
531 *Perkin Transaction 1*, 1433-1436.

- 532 8 Aatmani ME, Poujol S, Astre C, Malosse F, Pinguet F 2002. Stability of Dacarbazine in
533 Amber Glass Vials and Polyvinyl Chloride Bags. American Society of Health-System
534 Pharmacists, 59:1351-1356.
- 535 9 Islam MS, Asker AF 1994. Photostabilization of Dacarbazine with Reduced Glutathione.
536 Parenteral Drug Association Journal of Pharmaceutical Science and Technology, 48:38-40.
- 537 10 Lunn G, Rhodes SW, Sansone EB, Schmuff NR 1994. Photolytic Destruction and Polymeric
538 Resin Decontamination of Aqueous Solutions of Pharmaceuticals, Journal of
539 Pharmaceutical Sciences, 83(9):1289-1293.
- 540 11 Shetty BV, Schowen RL, Slavik M, Riley CM 1992. Degradation of Dacarbazine in Aqueous
541 Solution, Journal of Pharmaceutical & Biomedical Analysis, 10(9):675-683.
- 542 12 Piechocki JT, Thoma K 2010. Pharmaceutical Photostability and Photostabilisation
543 Technology. Informa Healthcare, London.
- 544 13 Tonnesen HH 2004. Photostability of Drugs and Drug Formulations (second Edition). CRC
545 Press: London.
- 546 14 Maafi M, Brown RG, 2007. The kinetic model for AB(1 Φ) systems. A closed-form
547 integration of the differential equation with a variable photokinetic factor. J. Photochem.
548 Photobiol. A: Chem., 187, 319-324.
- 549 15 Maafi M 2010. The potential of AB(1 Φ) systems for direct actinometry. Diarylethenes as
550 successful actinometers for the visible range. Phys. Chem. Chem. Phys. 12, 13248–13254.
- 551 16 Maafi W, Maafi M 2013. Modelling Nifedipine Photodegradation, Photostability and
552 Actinometric Properties. Int. J. Pharm., 456, 153-164.

- 553 17 Maafi M, Maafi W 2014. Φ -order kinetics of photoreversible drug reactions. *Int. J. Pharm.*,
554 471, 536-543.
- 555 18 Maafi M, Maafi W 2014. Montelukast photodegradation: Elucidation of Φ -order kinetics,
556 determination of quantum yields and application to actinometry. *Int. J. Pharm.*, 471, 544-
557 552.
- 558 19 Maafi M, Brown RG 2008. Kinetic analysis and kinetic elucidation options for AB(1k,2 Φ)
559 systems. New spectrokinetic methods for photochromes. *Photochem. Photobiol. Sci.*, 7,
560 1360–1372.
- 561 20 Dyer JR 1965. *The application of absorption spectroscopy of organic compounds*. Prentice-
562 Hall, London.
- 563 21 Sathyanarayana DN 2001. *Electronic Absorption Spectroscopy and Related Techniques*.
564 University Press, Hyderabad, India.
- 565 22 Maafi M, Lee LY 2015. Actinometric and Φ -order photodegradation properties of anti-
566 cancer Sunitinib. *J. Pharm. Biomed. Anal.*, 110, 34–41.
- 567 23 Maafi M, Maafi W 2015. Quantitative assessment of photostability and photostabilisation
568 of Fluvoxamine and its design for actinometry. *Photochem. Photobiol. Sci.*, 14(5), 982-994.
- 569 24 Maafi M, Maafi W 2015. Quantification of Unimolecular Photoreaction Kinetics:
570 Determination of Quantum Yields and Development of Actinometers—The
571 Photodegradation Case of Cardiovascular Drug Nisoldipine. *Int. J. Photoenergy*. *In press*.
- 572 25 Montalti M, Credi A, Prodi L, Gandolfi MT 2006. *Handbook of Photochemistry*. Third ed.
573 CRC Press – Taylor & Francis, Boca Raton, London, New York.

- 574 26 Kuhn HJ, Braslavsky SE, Schmidt R 2004. Chemical actinometry. *Pure Appl. Chem.* 76, 2105–
575 2146.
- 576 27 ICH, 1996. Guidance for industry Q1B photostability testing of new drug substances and
577 products. *Fed. Regist.* 62, 27115-27112.
- 578 28 De Azevedo Filho CA, De Filgueiras Gomes D, De Melo Guedes JP, Batista RMF, Santos BS
579 2011. Considerations on the quinine actinometry calibration method used in photostability
580 testing of pharmaceuticals. *J. of Pharm. and Biomed. Anal.* 54, 886-888.
- 581 29 Baertschi SW, Alsante KM, Tonnesen HH, 2010. A critical assessment of the ICH guideline
582 on photostability testing of new drug substances and products (Q1B): recommendation for
583 revision. *J. Pharm. Sci.* 99, 2934-2940.
- 584 30 Baertschi SW 1997. Commentary on the quinine actinometry system described in the ICH
585 draft guideline on photostability testing of new drug substances and products. *Drug*
586 *Stability.* 1, 193-195.
- 587 31 Allen JM, Allen SK, Baertschi SW 2000. 2-Nitrobenzaldehyde: A Convenient UV-A and UV-B
588 Chemical Actinometer for Drug Photostability Testing. *J. Pharm. Biomed. Anal.* 24, 167-178.
589
590
591